

Highly-Selective Ridge Gap Waveguide Based Filters for Multi-Band Satellite Applications

Neetirajsinh J. Chhasatia^{1, *}, Jitendra P. Chaudhari¹, and Amit V. Patel²

Abstract—In this paper, a pioneering and innovative approach for multiple-band ridge gap waveguide (MB-RGW) based narrowband bandpass filter for satellite applications is presented. The MB-RGW represents a significant and emerging technological advancement within the domain of microwave and millimeter-wave engineering. It comprises a periodic structure that enables the propagation of electromagnetic waves along its axis. We have provided a detailed analysis of the MB-RGW, which includes its design, simulation, and experimental results. A prototype filter, designed according to specifications, was successfully produced with a fabricated circuit area measuring $42.25 \text{ mm} \times 76.25 \text{ mm} \times 8.8 \text{ mm}$. We demonstrate that the MB-RGW can achieve multiple bands with a single structure, making it a versatile and efficient device for a wide range of applications. We also present a detailed analysis of the factors that affect the performance of the MB-RGW, including the geometry of the ridge and the spacing between ridges. Our experimental results show that the MB-RGW can achieve high levels of attenuation and isolation, making it a promising candidate for the use in microwave and millimeter-wave circuits and systems. The experimental results show S_{11} smaller than -20 dB over relative bandwidths, and S_{21} has a maximum of -0.07 dB . The proposed filter demonstrates four resonances at frequencies of 10.6 GHz , 12.6 GHz , 14.7 GHz , and 17.1 GHz , catering to mobile and fixed radio locations as well as satellite applications. It exhibits a fractional bandwidth of 0.44% at 3 dB in the X-Band and approximately 0.57% to 0.61% at 3 dB bandwidth in the Ku-band. The filter offers a compact, cost-effective, and easily implementable solution for satellite communication systems, including space operations, earth exploration, satellite TV broadcasting, and fixed satellite services (FSS). Overall, this paper provides a comprehensive overview of the MB-RGW and its potential for the use in a range of applications.

1. INTRODUCTION

The need for faster data speeds in short-range wireless communications, combined with the limited availability of frequencies, has led both industry professionals and researchers to focus on high frequencies, specifically millimeter wave spectrum. This expanded portion of the spectrum has generated significant interest in the development of commercial mm-wave communication systems. Higher frequencies facilitate the downsizing of RF components, including filters, resulting in the development of compact modules that integrate active and passive elements with filters within a single package.

Nonetheless, the integration of interconnected transmission lines and passive components within these modules presents considerable obstacles when they operate at millimeter wave frequencies, specifically when conventional technologies such as microstrip transmission lines and waveguides are used. Microstrip transmission lines encounter significant losses, encompassing both dielectric and

Received 30 June 2023, Accepted 25 July 2023, Scheduled 5 August 2023

* Corresponding author: Neetirajsinh Jaydeepsinh Chhasatia (neetiraj.n.c@ieee.org).

¹ V.T. Patel Department of Electronics & Communications, Chandubhai S Patel Institute of Technology, Charotar University of Science and Technology, Changa, Anand, Gujarat 388421, India. ² Wolfson School of Mechanical, Electrical and Manufacturing Engineering, Loughborough University, Thurmaston, England, LE11 3TU, United Kingdom.

conductive elements, thereby impairing overall performance. On the other hand, waveguides pose challenges in terms of their compatibility with integrated circuits and necessitate meticulous assembly processes to establish reliable electrical contacts, especially when being assembled as distinct blocks. Consequently, the development of innovative technologies becomes imperative to overcome these challenges imposed by upcoming next-generation systems.

The gap waveguide technology [24] is a recent and promising solution to address challenges encountered in millimeter wave applications using conventional technologies. This innovative component enables the controlled guidance of the electromagnetic field along desired directions within the gap between metal plates while preventing propagation along undesired directions. As a result, it effectively eliminates leakage and unwanted radiations that may occur in circuits with subpar metal contacts.

The Ku-band ridge gap waveguide bandpass filter finds widespread applications across diverse industries, making it a versatile and crucial component in modern communication and radar systems. These filters are extensively employed in satellite communication systems, enabling efficient transmission and reception of signals within the Ku frequency range (12–18 GHz). Additionally, they play a crucial role in radar systems, enhancing target detection, tracking, and imaging capabilities. Moreover, the Ku-band filters have significant relevance in wireless communication, supporting high-data-rate applications such as point-to-point microwave links and wireless backhaul, and are even utilized in millimeter-wave backhaul solutions for 5G networks, addressing the growing data traffic demands of 5G base stations. Beyond communication, these filters contribute to scientific endeavors, supporting radio astronomy research and remote sensing applications. They also find application in industrial and defense settings for critical signal processing tasks.

In light of these broad-ranging applications, we have undertaken an in-depth analysis to highlight the unique attributes of the proposed filter. We have demonstrated its potential for reduced size, improved insertion loss, higher power-handling capabilities, and cost-effectiveness compared to conventional filters. Furthermore, our work provides detailed insights into how this innovation can positively impact various Ku-band systems, such as satellite communication and radar. By doing so, we aim to emphasize the practical significance of our research and underscore its relevance in advancing the state-of-the-art in Ku-band technology, further solidifying the value of our contribution to this field.

This achievement is made possible by incorporating an Artificial Magnetic Conductor (AMC) around a metal ridge/strip or groove [29, 30]. By implementing a bed of nails structure, consisting of a textured layer beneath an upper metal lid, the gap waveguide effectively suppresses all parallel-plate modes. This configuration enables selective propagation solely within the air gap formed between the ridge/strip and the upper plate.

This paper focuses on the development of MB-RGW, encompassing the design of unit cells, dispersion diagram analysis, and the development of a toothed ridge structure. This structure is particularly appealing for both low and high-frequency applications, as it allows propagation in the air while maintaining low losses. The simulated results and experimental validations further support the effectiveness of the proposed MB-RGW.

The experimental validations demonstrate the MB-RGW's exceptional performance with minimal losses. The incorporation of an Artificial Magnetic Conductor (AMC) [31] surface within the gap waveguide effectively eliminates leakage from the minute gaps between the metal plates, which is especially advantageous at high frequencies. The remarkable capabilities of the MB-RGW make it a highly viable solution for X/Ku band applications, including Mobile & Fixed Radio Location, Direct Broadcast Service (DBS), and both receiving and transmitting modes of Fixed Satellite Service (FSS). Its suitability for these specific frequency bands enables efficient and reliable performance in various communication systems, underscoring its potential impact in the field.

2. UNIT CELL DESIGN

Multiple bands Ridge Gap Waveguide (MB-RGW) filters have emerged as a promising periodic structure for selective waveguiding and filtering in microwave and millimeter-wave applications. Unlike conventional filters, MB-RGW filter offers a distinct advantage by eliminating the need for a substrate other than air [10, 14, 27]. This exceptional characteristic positions it as a superior choice for applications in air-based environments. The absence of an additional substrate minimizes losses and enables efficient

filtering performance in such scenarios. This feature simplifies the fabrication process and reduces the complexity and cost of the device. The MB-RGW filter has the potential to be employed in a variety of applications, including radar systems, wireless communication, satellite communication, and other microwave and millimeter-wave applications [3, 17, 22].

In the design of the MB-RGW filters, the process begins with the analysis of the dispersion diagram of a unit cell to determine the desired characteristics [7, 9]. Based on this analysis, the filter is designed accordingly. To evaluate the performance of the filter, numerical simulations are conducted, and the results are compared with the desired specifications. Subsequently, the filter is fabricated and measured to validate the simulated results, ensuring the accuracy and effectiveness of the design.

Started with the unit cell development, by defining the stopband based on lower and upper cut-off frequencies, a metallic pin can function as a high-impedance surface within this defined frequency range. The height of metallic pin determines the lower cut-off frequency, while the sum of pin height and air gap distance determines the upper cut-off frequency, which should be half of the wavelength ($\lambda/2$).

A periodic infinite unit pin cell [11, 25] exhibits a dispersion diagram that can be used to determine the stopband frequency range. The stop bandwidth is inversely proportional to the air gap distance between the pin and upper metal lid. A smaller air gap distance leads to a wider stopband. The metallic pin structure can be electrically modeled as a resonant parallel LC circuit, whose impedance is equal to the impedance of parallel LC circuit.

At the resonant frequency, the impedance of the parallel LC circuit is maximized, and the proposed structure — an infinite periodic unit cell inside a parallel plate structure — provides the stopband. The computed dispersion diagram for an infinite two-dimensional pin array is presented in Fig. 1.

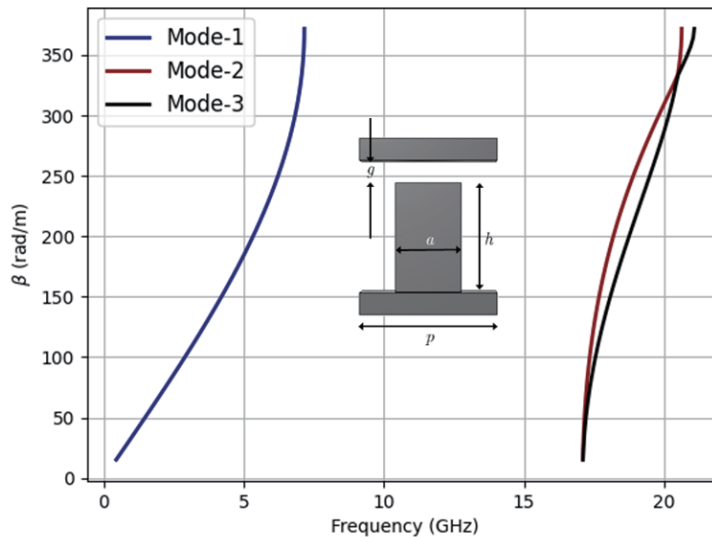


Figure 1. The dispersion diagram showcasing various modes ($p = 8.45$ mm, $h = 6.5$ mm, $a = 3.9$ mm, $g = 1.3$ mm).

Periodic structures are a vital aspect of transmission line and waveguide systems, characterized by the presence of reactive elements at regular intervals along the structure [6, 28]. These elements can manifest in various forms, depending on the specific type of transmission line employed. The reactive components often arise from discontinuities within the line, although they can also be represented as reactances along the transmission line itself. To gain insights into the fundamental wave propagation phenomena associated with periodic structures [23, 26], it is instructive to analyze a simplified structure as depicted in Fig. 2. In this particular configuration, each unit cell of the transmission line represents a segment of length “ d ” that encompasses a shunt susceptance “ B ”. Notably, these values are normalized with respect to the characteristic impedance “ Z_0 ” of the transmission line. Considering the unit cell as a two-port network, it becomes possible to establish a relationship between the voltages and currents on either side of the n th periodic structure unit cell by means of the ABCD matrix. The ABCD

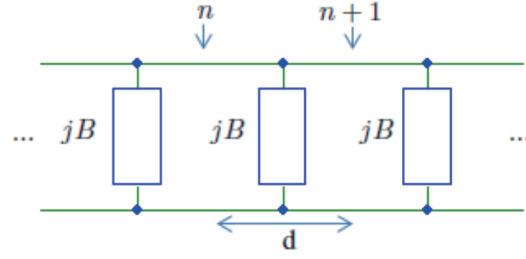


Figure 2. A transmission line that incorporates periodically placed lumped elements.

matrix serves as a powerful analytical tool in the realm of transmission line analysis. It facilitates the characterization of how input and output voltages and currents are interrelated within a network. By studying the behavior of periodic structures through the analysis of their ABCD matrices, researchers can gain a deeper understanding of wave propagation phenomena and how the presence of reactive elements impacts the characteristics of the transmission line system.

The load elements within the transmission line are typically created through intentional discontinuities introduced into the line. However, for analytical purposes, these load elements can be represented as reactances distributed along the transmission line. In the present investigation, we focus on a simplified structure, as depicted in Fig. 2, aiming to grasp the fundamental principles underlying the wave propagation phenomenon in periodic structures. In this particular configuration, each unit cell of the transmission line encompasses a length d and is centered around a shunt susceptance B , which is normalized relative to the characteristic impedance Z_0 .

By regarding the unit cell as a two-port network, we can establish a relationship between the voltages and currents present on each side of the n th unit cell within the periodic structure. This relationship can be expressed using the ABCD matrix, which encapsulates the transmission characteristics of the unit cell [1, 4].

$$\begin{bmatrix} V_n \\ I_n \end{bmatrix} = \begin{bmatrix} a & b \\ c & d \end{bmatrix} \begin{bmatrix} V_{n+1} \\ I_{n+1} \end{bmatrix} \quad (1)$$

$$A = \left(\cos \theta - \frac{\bar{B}}{2} \sin \theta \right) \quad (2)$$

$$B = j \left(\sin \theta + \frac{\bar{B}}{2} \cos \theta - \frac{\bar{B}}{2} \right) \quad (3)$$

$$C = j \left(\sin \theta + \frac{\bar{B}}{2} \cos \theta + \frac{\bar{B}}{2} \right) \quad (4)$$

$$D = \left(\cos \theta - \frac{\bar{B}}{2} \sin \theta \right) \quad (5)$$

where the matrix parameters A , B , C , and D can be determined by cascading three distinct sections. Firstly, a transmission line segment with a length of $\frac{d}{2}$ is connected to the initial port. This is followed by a shunt susceptance B , and subsequently, another transmission line segment with a length of $\frac{d}{2}$ is connected to the final port. The combination of these three sections leads to the determination of the matrix parameters A , B , C , and D , which capture the transmission properties of the overall structure.

In this context, the variable θ represents the electrical length of the transmission line within the unit cell, which is directly related to the propagation constant k of the unloaded line. It is important to note that the product of matrix parameters AD and BC , $AD - BC = 1$, as mandated by the reciprocity of networks. Assuming an infinite periodic structure, the voltage and current at the n th terminals should be equivalent to those at the $(n + 1)$ th terminals. However, due to the propagation along the cell, there is a phase delay introduced between the two sets of voltage and current [15]. So, we have

$$\begin{bmatrix} V_{n+1} \\ I_{n+1} \end{bmatrix} = e^{-\gamma z} \begin{bmatrix} V_n \\ I_n \end{bmatrix} \quad (6)$$

Thus

$$AD + e^{2\gamma d} - (A + D)e^{\gamma d} - BC = 0 \quad (7)$$

and as we have taken the reciprocal network case, $AD - BC = 1$ and putting the values of A and B , we get

$$\cosh \gamma d = \cos \theta - \frac{\bar{B}}{2} \sin \theta \quad (8)$$

When the magnitude of $\cos \theta - \frac{\bar{B}}{2} \sin \theta < 1$ is less than one, it indicates that α equals zero and $\gamma = j\beta$. Consequently, in such a scenario, the periodic structure facilitates the propagation of a wave. Conversely, if the magnitude of $\cos \theta - \frac{\bar{B}}{2} \sin \theta$ exceeds one, it implies that no wave can propagate along the structure.

The geometry of RGW structure, including the ridge and gap widths and heights, significantly affects the filter's performance. The filter's performance can be improved by manipulating the RGW structure's geometry, leading to a more efficient and optimized filter. In addition, various numerical techniques can be used to accelerate the design and analysis process, providing a more comprehensive understanding of the filter's behavior.

In this paper, toothed ridge is introduced aiming the operating frequency in the X and Ku band ranges, and experiment shows its characteristics as high performance and compact size. The toothed ridge provides a reflective surface that can support multiple band and multiple mode behavior, which allows for the design of complex and highly selective filters. By adjusting the size and spacing of the teeth, it is possible to create a range of resonant modes that can be selectively coupled to achieve the desired frequency response. Furthermore, the use of toothed ridges can also reduce the coupling between adjacent resonators, thereby improving the filter performance. Hence, it offers a powerful design tool for achieving high-performance microwave and millimeter-wave filters with multiple bands and modes.

Figure 3 shows the geometry of the full structure containing bed of nails, toothed ridge.

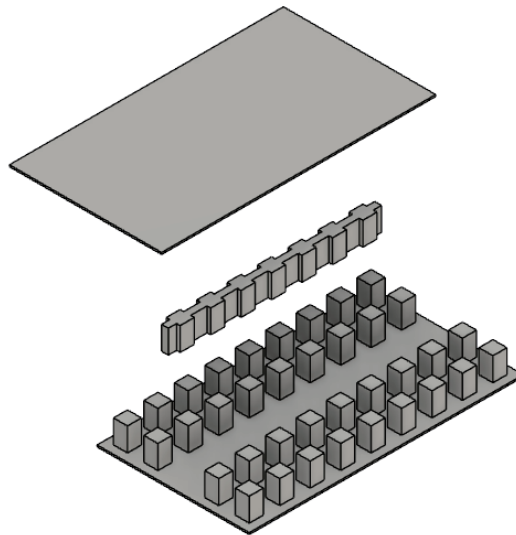


Figure 3. A comprehensive perspective view of the entire geometry, featuring a bed of nails underneath.

Once the ridge and gap dimensions are determined, the full-wave simulations of the subarray have been conducted using the finite-element method, specifically employing the Time-Domain Solver.

3. DESIGN OF MULTI-BAND (X-KU BAND) RGW STRUCTURE

The proposed geometry of the MB-RGW involves the field propagation along a ridge situated on the textured surface of metal pins, as depicted in Fig. 3. Unlike standard rectangular waveguides, there is

no need for electrical contact between the walls in an RGW. The selection of appropriate pin dimensions and gap size is crucial for achieving a stopband between 7 and 18 GHz.

The proposed bandpass filter is composed of a specific geometric configuration and schematic diagram [6], as illustrated in Fig. 4. The filter incorporates toothed ridge surrounded by pins. The base part of the ridge is varied for fine-tuning the multiple modes in multiple frequency bands. Selectivity of the frequency is determined by the LC structure created in the ridge, i.e., interspace of the inductive windows. The value of equivalent of one of the lumped elements can be given as $f = \omega_0/2\pi = 1/2\pi\sqrt{LC}$.

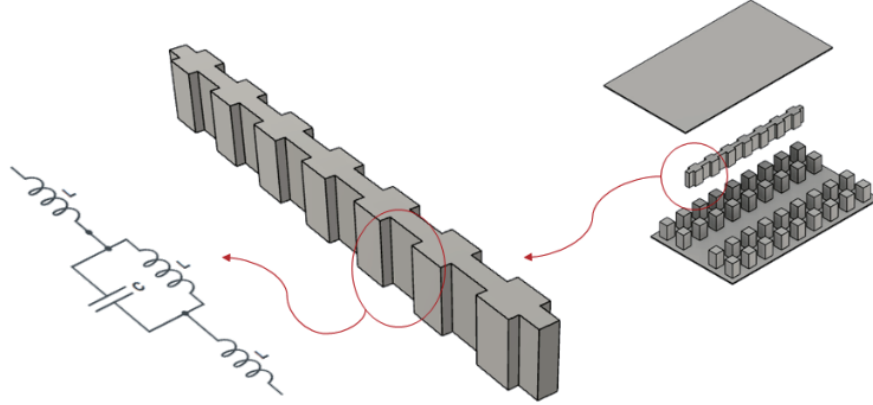


Figure 4. Comprehensive geometry perspective with underlying bed of nails, accompanied by simplified LC circuit representation.

The width of the base of toothed ridge plays a crucial role in fine-tuning the S -parameters of the proposed structure, as demonstrated in Fig. 5. Reducing the central width of the ridge results in shifting left in the frequency axis. Frequency fine tuning can be done using this structure.

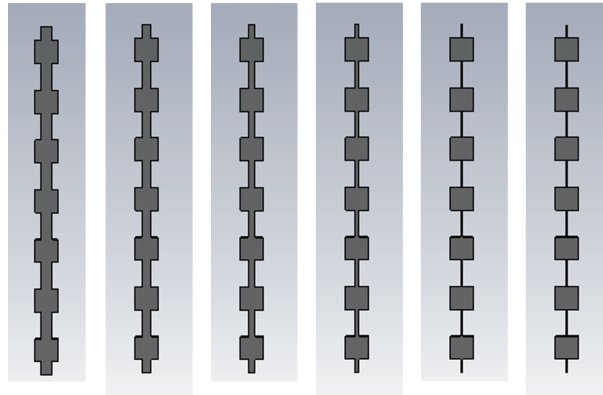


Figure 5. Width variation of the toothed ridge: Thick to Thin.

To investigate the impact of varying the width of the base of ridge on frequency selectivity and the fine-tuning of S -parameters, a systematic analysis was conducted. The width of the base was incrementally adjusted within the range of 1 mm to 2 mm. Starting from an initial width of 1 mm, gradual and controlled variations were made, gradually increasing towards the upper limit of 2 mm. This approach allowed for the examination of the effects of different widths on the desired frequency response and the fine-tuning of the S -parameters within the specified frequency range as shown in Fig. 6. With reference to Fig. 5, it can be observed that an increase in the base width of the toothed ridge shifts the selectivity towards the higher frequency side, as depicted in Fig. 6. Consequently, this

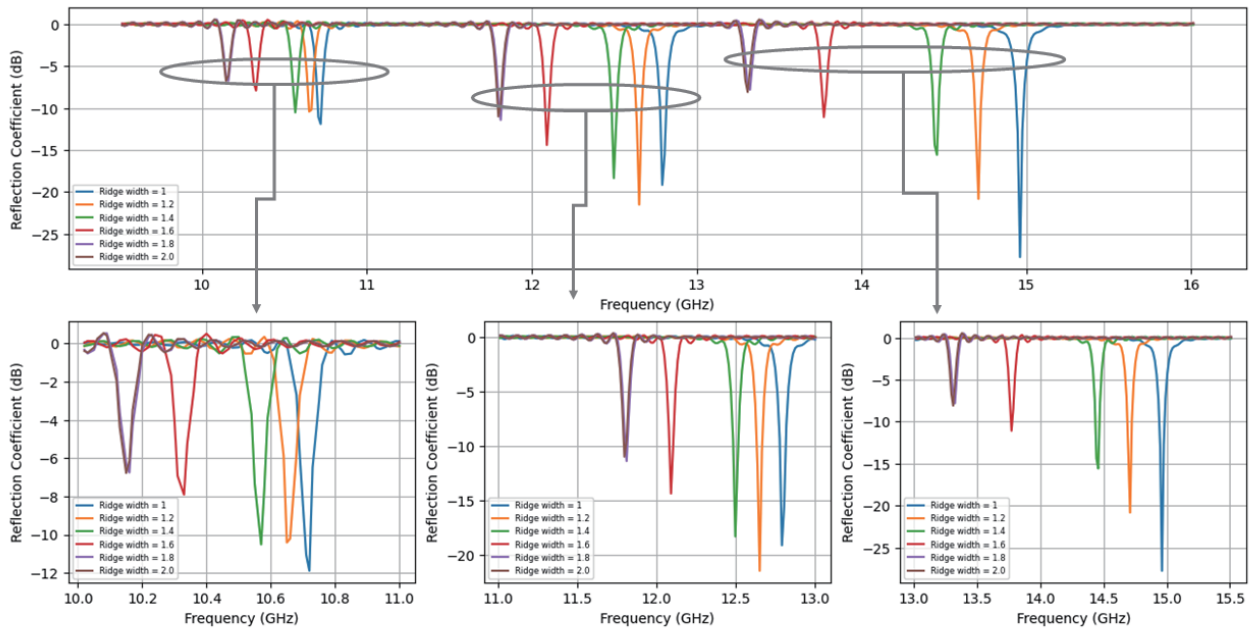


Figure 6. Simulated S_{11} of the filter with notch frequency tuning. Reflection and transmission coefficient response of the toothed ridge structure (MB-RGW).

fine-tunes the selectivity of the multiband filter. Altering the base width of the toothed ridge by just 1 millimeter (mm) can have a notable influence on the frequency response of the multi-band filter. To be precise, this small 1 mm variation has the potential to cause a frequency shift of ~ 0.5 gigahertz (GHz) on the scale used for measurement. The magnitude of this frequency shift demonstrates the sensitivity of the multiband filter’s performance to even minor adjustments in its physical dimensions. Such precise control over the frequency response allows for fine-tuning the filter’s selectivity to cater to specific requirements and optimize its performance in various satellite applications, particularly those involving multiple frequency bands and signal filtering.

The dimensions of the entire structure, as portrayed in Fig. 3, have been conclusively established and are outlined in Table 1. Moreover, a comparative analysis of crucial parameters with respect to pertinent literature [20] is presented in Table 3. The filter design, implemented at a frequency of 14 GHz, was accomplished utilizing CST Microwave Studio (MWS). The simulated outcomes of the Insertion Loss and Return Loss for the aforementioned design are visually represented in Fig. 7. The distinctive bandpass regions have been correlated with specific applications in Table 2, as referenced in researches. To ensure the accuracy of the simulation results, experimental measurements were conducted for validation. Fig. 9 shows an overview of the fabricated filter, featuring dimensions of $42.25 \text{ mm} \times 76.25 \text{ mm} \times 8.8 \text{ mm}$, produced via conventional milling techniques. The evaluation of the reflection coefficient of the filter structure was done using an Agilent network analyzer operating in the mmWave band. The comparison between the simulated and measured results for the complete structure is illustrated in Fig. 10. Observe that within desired operating range, the simulated reflection is less than -20 dB , while the insertion loss is less than 0.05 dB . Significant agreement has been achieved between measurement and simulation results. Discrepancies observed between simulated and measured

Table 1. Dimension of unit cell for desired frequency.

Period (p)	Pin height (h)	Air Gap (g)	Width (a)	Desired Stop band
$\lambda/4$	$\lambda/5$	$\lambda/24$	$\lambda/8$	7–17 GHz

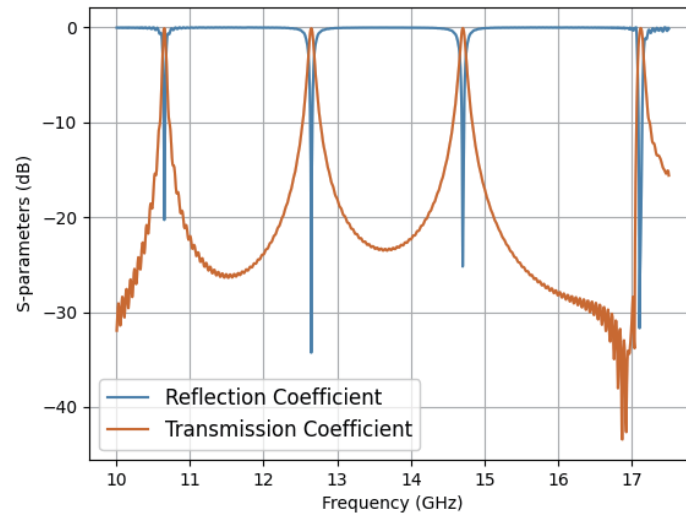


Figure 7. Reflection and transmission coefficient response of the toothed ridge structure (MB-RGW).

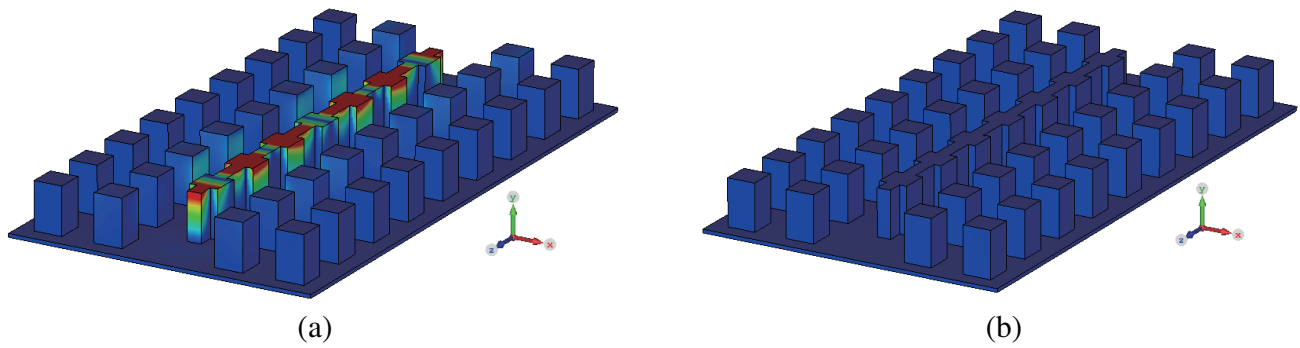


Figure 8. Simulated electric field distribution analysis of the proposed filter at different frequencies. (a) E -field distribution within the desired frequency in a ridge gap waveguide filter. (b) E -field distribution at undesired frequency in a ridge gap waveguide filter.

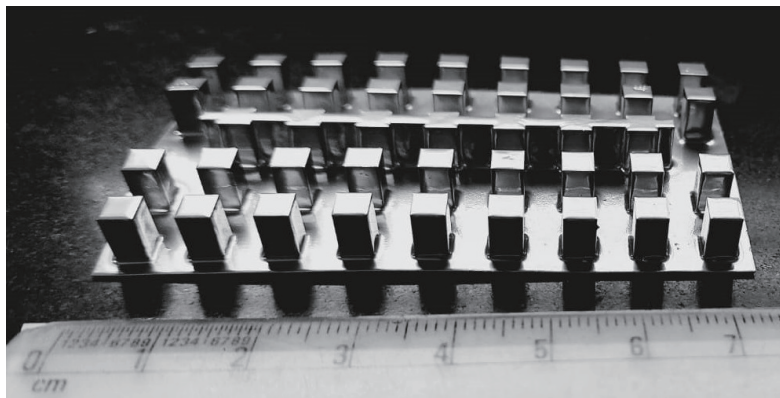


Figure 9. Photograph of fabricated filter prototype.

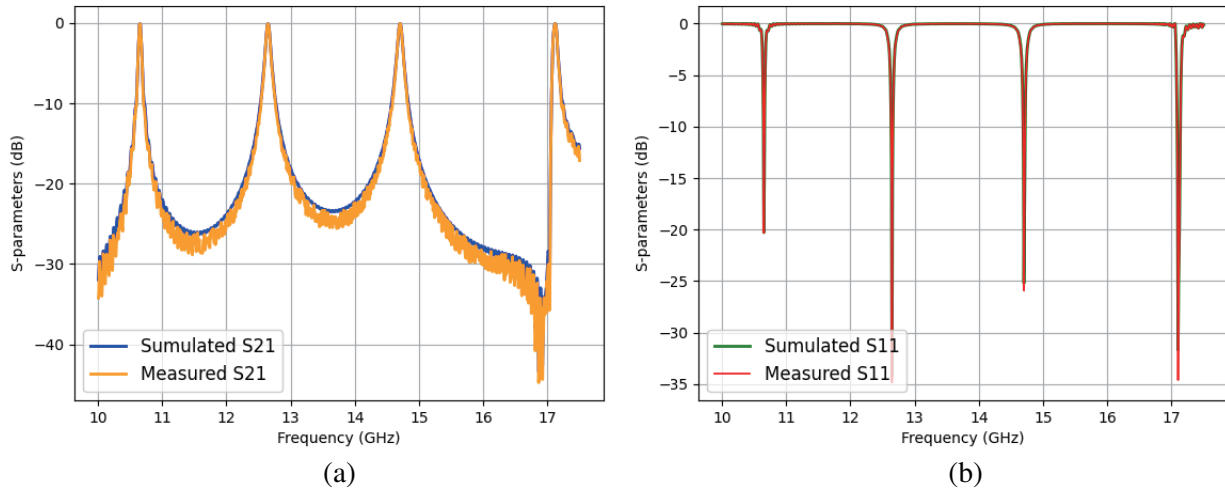


Figure 10. Measured & Simulated S -parameter response of the filter with toothed ridge. (a) Measured & Simulated S_{21} response of the filter with toothed ridge. (b) Measured & Simulated S_{11} response of the filter with toothed ridge.

Table 2. Filter characteristics: application, bandwidth, fractional bandwidth, and operating range.

Frequency (GHz)	Bandwidth (GHz)	Fractional Bandwidth (%)	Application	Band
10.6	0.04	0.44	Mobile & Fixed Radio Location	X-Band
12.6	0.07	0.61	DBS & FSS	Ku-Band
14.7	0.08	0.57	DBS & FSS	Ku-Band
17.1	0.08	0.49	DBS & FSS	Ku-Band

Note: FSS & DBS: Fixed Satellite Service in receive & transmit mode, and Direct Broadcast Service in receive mode [5, 12, 16, 18].

Table 3. Comparison of the proposed design with existing literature.

Parameter	Length	Substrate	Presence of Dielectric	Characteristics	S_{11}	S_{21}	Remarks
[21]	$2.61 \times \lambda_g$	Roger (R04003)	Yes	Single-Band	-10 dB	-1.35 dB	Wide-band
[20]	$2.37 \times \lambda_g$	Arlon (AD300A)	Yes	Multi-Band	-30.94 dB	-0.21 dB	Narrow-band
[19]	$2.24 \times \lambda_g$	Taconic TLT™	Yes	Single-Band	-30 dB	-1.7 dB	Narrow-band
[13]	$1.34 \times \lambda_g$	PTFE	Yes	Single-Band	-25.4 dB	-1.15 dB	Wide-band
[8]	$7.22 \times \lambda_g$	Air	No	Single-Band	-16.78 dB	-12 dB	Narrow-band
[2]	$3.23 \times \lambda_g$	Air	No	Single-Band	-16.38 dB	-0.15 dB	Narrow-band
This Work	$2.03 \times \lambda_g$	Air	No	Multi-Band	-35 dB	-0.07 dB	Narrow-band

outcomes can be attributed to inherent variations stemming from assembly tolerances and fabrication inaccuracies. The electric field distributions within the structure were observed at frequencies of 12.6 GHz (desired) and 13.6 GHz (undesired) and are depicted in Fig. 8(a) and Fig. 8(b). Experimental observations substantiate the propagation of the EM wave within the designated bandpass frequency range, accompanied by its effective suppression at frequencies falling outside the specified range.

4. CONCLUSION

A pioneering multiple-band ridge gap waveguide (MB-RGW) filter has been put forth and subsequently validated through experimental analysis, leveraging the toothed ridge gap waveguide technology. The resonant frequency of the filter has been fine-tuned by optimizing the dimensions of the toothed cavities. The proposed filter exhibits an insertion loss of less than 0.05 dB within the X-Ku frequency bands, as determined from the measured results. The comprehensive examination of the filter and transition components reveals highly encouraging overall performance characteristics, validating their efficacy and potential for application in microwave communication systems, and this structure shows potential for a wide range of communication and sensing applications in the X and Ku frequency bands. By following the design and simulation methodology outlined in this paper, the RGW can be tailored to meet specific stopband requirements in these frequency ranges. This paper provides a useful reference for researchers and engineers involved in the design of waveguides for X and Ku band applications. The proposed model is vital for high-capacity, short-range 5G communication. Microwave filters at these frequencies remove unwanted signals, ensuring clean transmission and reception. They facilitate efficient satellite communication and long-distance wireless links. These filters find applications in remote sensing and radar, isolating desired signals for accurate analysis. Further research could explore additional optimization techniques for RGW designs to further enhance their performance in these and other frequency ranges.

REFERENCES

1. Shi, Y. and H. J. Wang, "Dual-ridge gap waveguide-based antenna with diverse beam capabilities," *IEEE Open Journal of Antennas and Propagation*, Vol. 3, 774–782, 2022, doi: 10.1109/OJAP.2022.3190225.
2. Chhasatia, N., J. Chaudhari, and A. Patel, "Ridge gap waveguide based band pass filter for Ku-band application," *IOP Conference Series: Materials Science and Engineering*, Vol. 1206, No. 1, 012011, 2021, doi: 10.1088/1757-899X/1206/1/012011.
3. Pizarro, F., C. Sanchez-Cabello, J. L. Vazquez-Roy, and E. Rajo-Iglesias, "Considerations of impedance sensitivity and losses in designing inverted microstrip gap waveguides," *AEU Int. J. Electron. Commun.*, Vol. 124, 153353, 2020.
4. Huang, H., Y. Wu, W. Wang, W. Feng, and Y. Shi, "Analysis of the propagation constant of a ridge gap waveguide and its application of dual-band unequal couplers," *IEEE Transactions on Plasma Science*, Vol. 48, No. 12, 4163–4170, Dec. 2020, doi: 10.1109/TPS.2020.3034669.
5. Thaher, R. H. and S. H. M. jassim, "Design of dual band elliptical microstrip antenna for satellite communication," *IOP Conference Series: Materials Science and Engineering*, Vol. 928, 022066, 2020.
6. Zhang, T., L. Chen, S. M. Moghaddam, A. Uz Zaman, and J. Yang, "Wideband dual-polarized array antenna on dielectric-based inverted microstrip gap waveguide," *Proceedings of the 2019 13th European Conference on Antennas and Propagation (EuCAP)*, 1–3, Krakow, Poland, March 31–April 5, 2019.
7. Birgermajer, S., N. Janković, V. Crnojevic-Bengin, and V. Radonić, "Millimeter-wave dual-mode filters realized in microstrip-ridge gap waveguide technology," *J. Infrared Millim. Terahertz Waves*, Vol. 40, 92–107, 2019.
8. Wu, T., T. Zhang, and J. Huang, "Design of Ku-band size-reduced waveguide slot filter antenna loaded with metal ridges," *Journal of Physics: Conference Series*, Vol. 1325, No. 1, 012199, 2019, doi: 10.1088/1742-6596/1325/1/012199.

9. Ali, M. M., S. I. Shams, and A. R. Sebak, "Low loss and ultra flat rectangular waveguide harmonic coupler," *IEEE Access*, Vol. 6, 38736–38744, 2018.
10. Liu, J., J. Yang, and A. U. Zaman, "Study of dielectric loss and conductor loss among microstrip, covered microstrip and inverted microstrip gap waveguide utilizing variational method in millimeter waves," *Proceedings of the 2018 International Symposium on Antennas and Propagation (ISAP)*, 1–2, Busan, Korea, October 23–26, 2018.
11. Rajo-Iglesias, E., M. Ferrando-Rocher, and A. U. Zaman, "Gap waveguide technology for millimeter-wave antenna systems," *IEEE Commun. Mag.*, Vol. 56, 14–20, 2018.
12. Afolayan, B. O., T. J. Afullo, and A. Alonge, "Subtropical rain attenuation statistics on 12.6 GHz Ku-band satellite link using synthetic storm technique," *SAIEE Africa Research Journal*, Vol. 109, No. 4, 230–236, Dec. 2018, doi: 10.23919/SAIEE.2018.8538336.
13. Muchhal, N., A. Chakraborty, M. Vishwakarma, and S. Srivastava, "Slotted folded substrate integrated waveguide band pass filter with enhanced bandwidth for Ku/k band applications," *Progress In Electromagnetics Research M*, Vol. 70, 51–60, 2018, doi: 10.2528/PIERM18041804.
14. Liu, J., A. Vosoogh, A. U. Zaman, and J. Yang, "Design and fabrication of a high-gain 60-GHz cavity-backed slot antenna array fed by inverted microstrip gap waveguide," *IEEE Trans. Antennas Propag.*, Vol. 65, 2117–2122, 2017.
15. Shams, S. I. and A. A. Kishk, "Design of 3-dB hybrid coupler based on RGW technology," *IEEE Trans. Microw. Theory. Tech.*, Vol. 65, 3849–3855, October 2017.
16. Kandönmez, Ş, O. Kolancıoğlu, D. H. Boyacı, M. E. Koca, and T. İmeci, "High gain perturbed pentagonal shaped diamond slotted patch antenna at 17.1 GHz," *2017 International Applied Computational Electromagnetics Society Symposium — Italy (ACES)*, 1–2, Firenze, Italy, 2017.
17. Rajo-Iglesias, E. and A. A. Brazález, "5G antenna in inverted microstrip gap waveguide technology including a transition to microstrip," *Proceedings of the 2016 International Symposium on Antennas and Propagation (ISAP)*, 1042–1043, Okinawa, Japan, October 24–28, 2016.
18. Kuralay, E. N., E. F. Uzun, O. Ates, Y. M. Sahin, and T. İmeci, "Perturbed hexagonal antenna at 14.7 GHz," *2016 IEEE/ACES International Conference on Wireless Information Technology and Systems (ICWITS) and Applied Computational Electromagnetics (ACES)*, 1–2, Honolulu, HI, USA, 2016.
19. Huang, F., J. Zhou, and W. Hong, "Ku band continuously tunable circular cavity SIW filter with one parameter," *IEEE Microwave and Wireless Components Letters*, Vol. 26, No. 4, 270–272, April 2016, doi: 10.1109/LMWC.2016.2537785.
20. Patel, A., Y. Kosta, A. Vala, and R. Gosai, "Design and performance analysis of metallic posts coupled SIW-based multiband bandpass and bandstop filter," *Microwave and Optical Technology Letters*, Vol. 57, 1–5, 2015, doi: 10.1002/mop.29105.
21. Rhbanou, A., S. Mohamed, and S. Bri, "Design of K-band substrate integrated waveguide bandpass filter with high rejection," *Journal of Microwaves, Optoelectronics and Electromagnetic Applications*, Vol. 14, 155–169, 2015, doi: 10.1590/2179-10742015v14i2473.
22. Brazález, A. A., E. Rajo-Iglesias, J. L. Vázquez-Roy, A. Vosoogh, and P. Kildal, "Design and validation of microstrip gap waveguides and their transitions to rectangular waveguide, for millimeter-wave applications," *IEEE Trans. Microw. Theory Technology*, Vol. 63, 4035–4050, 2015.
23. Sanchez-Cabello, C. and E. Rajo-Iglesias, "Optimized self-diplexed antenna in gap waveguide technology," *Proceedings of the 2015 IEEE International Symposium on Antennas and Propagation USNC/URSI National Radio Science Meeting*, 460–461, Vancouver, BC, Canada, July 19–24, 2015.
24. Pucci, E., "Gap waveguide technology for millimeter wave applications and integration with antennas," Ph.D. dissertation, 2013.
25. Kildal, P., A. U. Zaman, E. Rajo-Iglesias, E. Alfonso, and A. Valero-Nogueira, "Design and experimental verification of ridge gap waveguide in bed of nails for parallel-plate mode suppression," *IET Microw. Antennas Propag.*, Vol. 5, 262–270, 2011.
26. Alfonso, E., et al., "New waveguide technology for antennas and circuits," *Waves Year*, Vol. 3, 65–75, 2011.

27. Rajo-Iglesias, E., A. U. Zaman, and P. Kildal, "Parallel plate cavity mode suppression in microstrip circuit packages using a lid of nails," *IEEE Microw. Wirel. Components Lett.*, Vol. 20, 31–33, 2010.
28. Zhang, Q., Y. Dong, and J. Cao, "Dual-mode bandpass filter using microstrip SIR at Ka band," *Proceedings of the 2009 Asia Pacific Microwave Conference*, 1401–1404, Singapore, December 7–10, 2009.
29. Kildal, P. S., E. Alfonso, A. Valero-Nogueira, and E. Rajo-Iglesias, "Local metamaterials-based waveguides in gaps between parallel metal plates," *IEEE Antennas and Wireless Propagation Letters*, Vol. 8, 84–87, 2009.
30. Kildal, P. S., "Three metamaterials-based gap waveguides between parallel metal plates for mm/submm waves," *Proceedings of the Third European Conference on Antennas and Propagation, EuCAP*, 28–32, 2009.
31. Sievenpiper, D., "High-impedance electromagnetic surfaces," Ph.D. dissertation, 1999.